
Ford, T.W. and Anissimova, N.P. and Meehan, C.F. and Kirkwood, P.A. (2015) Functional plasticity in the respiratory drive to thoracic motoneurons in the segment above a chronic lateral spinal cord lesion. Journal of Neurophysiology . ISSN 0022-3077 (In Press)

# FUNCTIONAL PLASTICITY IN THE RESPIRATORY DRIVE TO THORACIC MOTONEURONS IN THE SEGMENT ABOVE A CHRONIC LATERAL SPINAL CORD LESION

TW Ford, NP Anissimova, CF Meehan and PA Kirkwood

Sobell Department for Motor Neuroscience and Movement Disorders, UCL Institute of Neurology, Queen Square, London WC1N 3BG, UK.

Running title Respiratory drive in spinal cord injury

Key words
Spinal cord injury - Thoracic motoneurons – Respiratory drive - Plasticity

No of words 8,448 (main sections)

Correspondence Dr P.A. Kirkwood
Sobell Department
UCL Institute of Neurology
Queen Square
London WC1N 3BG
UK.

Tel. +44 (0)20 3448 4190
Fax. +44 (0)20 7813 3107
E-mail peter.kirkwood@ucl.ac.uk

## ABSTRACT

A previous neurophysiological investigation demonstrated an increase in functional projections of expiratory bulbospinal neurons (EBSNs) in the segment above a chronic lateral thoracic spinal cord lesion which severed their axons. We have now investigated how this plasticity might be manifested in thoracic motoneurons, by measuring their respiratory drive and the connections to them from individual EBSNs. In anesthetized cats, simultaneous recordings were made intracellularly from motoneurons in the segment above a left-side chronic (16 week) lesion of the spinal cord in the rostral part of T8, T9 or T10 and extracellularly from EBSNs in the right caudal medulla, antidromically excited from just above the lesion, but not from below. Spike-triggered averaging was used to measure the connections between pairs of EBSNs and motoneurons. Connections were found to have a very similar distribution to normal and were, if anything (non-significantly), weaker than normal, being present for 42/158 pairs, vs. 55/154 pairs in controls. The expiratory drive in expiratory motoneurons appeared stronger than in controls, but again not significantly so. Thus we conclude that new connections made by the EBSNs following these lesions were made to neurons other than alpha-motoneurons. However, a previously unidentified form of functional plasticity was seen, in that there was a significant increase in the excitation of motoneurons during post-inspiration, being manifest either in increased incidence of expiratory-decrementing respiratory drive potentials, or in an increased amplitude of the post-inspiratory depolarizing phase in inspiratory motoneurons. We suggest that this component arose from spinal cord interneurons.


## INTRODUCTION

Most effort in experimental spinal cord injury (SCI) studies has been directed at segments below a spinal lesion, where the questions have been focused on the loss of function (notably motor function) that occurs in these lower segments and its restoration. However, segments above the lesion also suffer effects of spinal cord injury. In these higher segments there will be loss of ascending inputs, both from the periphery and from local and propriospinal interneurons as well as possible changes in modulatory state (Becker & Parker, 2015). Descending interneurons (or those with bifurcating axons, with both ascending plus descending branches, Saywell et al. 2011) that are located within the segments above the injury may also suffer from the effects of axotomy or loss of their targets (Conta & Stelzner 2004; Conta et al. 2010, 2011). Furthermore in some instances, especially for human cervical SCI, changes in the neural circuits immediately rostral to the injury may be profoundly important for the degree of upper limb control available to the injured person (Fawcett, 2002): any repair strategy that might restore function by the equivalent of one segment might, for instance, add useful hand function to the control of only the proximal limb.

The present study is one of a series into the plasticity that naturally occurs in the segment above a lateral lesion of the thoracic spinal cord, the aim being to investigate the specificity of any new connections formed in these circumstances, without the complications inherent in either regeneration across a lesion or in the multi-synaptic interneuronal circuits that may be strengthened around a lesion (Bareyre et al. 2004; Arvanian et al. 2006; Courtine et al. 2008; for review see Flynn et al. 2011). Useful neurons for this purpose

are the expiratory bulbospinal neurons (EBSNs), which make direct connections to motoneurons in each thoracic segment (Saywell et al. 2007). One study from this laboratory has already shown that the physiologically-assessed projections of these neurons increase in the segment immediately above a lateral lesion that transected their axons (Ford et al. 2000). The experiments described here were devised to measure the specificity of connections that may be involved in these projections, namely the connections to different categories of motoneuron. However, while making these measurements, we noticed that there were some overall changes in the respiratory drive to the motoneurons, which comprise a different aspect of the functional plasticity. This paper describes both of these measurements. Preliminary results have appeared (Anissimova et al. 2000, 2001).

## METHODS

*Animals*.

Experiments were conducted according to UK legislation [Animals (Scientific Procedures) Act 1986] under Project and Personal Licences issued by the UK Home Office. The data come from 19 adult cats 17 male, initial weighs 2.2 – 4.5 kg. Control data came from acute experiments on uninjured animals previously described (Saywell et al. 2007).

*Spinal Lesions.*

Anesthesia was induced with ketamine and chlorpromazine (40 and 1 mg $kg^{-1}$, respectively) or with ketamine and acepromazine (36 mg $kg^{-1}$ and 0.12 mg $kg^{-1}$ respectively), I.M. (Ketaset, Fort Dodge Animal Health Ltd, Southampton, UK; acepromazine, C-Vet Veterinary Products, Grampian Pharmaceutical Ltd), and maintained with ketamine, I.V. (transcutaneous catheter in the cephalic vein) as required. The analgesic buprenorphine was administered (Vetergesic, 0.3 mg, S.C.) at the end of the surgery and usually also the next day. Heart rate was monitored using an esophageal electrode. Aseptic precautions were taken.

A dorsal midline incision was made and the paraspinal muscles were retracted from two mid-thoracic vertebrae. A partial laminectomy was made of the caudal end of the rostral of these two and usually also a small part of the left side at the rostral end of the other, so as to allow access to the cord at the rostral part of the caudal underlying segment (T8, T9 or T10: 7, 7 and 5 cats respectively). The dura was opened and either a no. 11 or a small optical scalpel blade was used to make a partial hemisection to the left side of the spinal cord, sparing the dorsal columns. It was aimed to make the lesion near or just caudal to the level of the most rostral dorsal root of that segment. This position spared the roots and dorsal root ganglion of the segment above (verified *post mortem* in all animals). The dura was folded back over the lesioned cord and the muscles closed in layers, applying Cicatrin (Glaxo Welcome) antibiotic between layers. The skin was closed with absorbable suture, a spray dressing (Opsite, Smith and Nephew, UK) was applied and an antibiotic (amoxicillin 150mg, I.M.) was administered.

Functional recovery was monitored carefully thereafter, especially for the first few days following the operation. Bowel function was restored in most animals by the morning of D3, in all by D4, standing on 4 legs mostly by D3, in all by D6, walking using 4 legs mostly by D4, in all by D7 and a near normal gait by all within 3 weeks (D0 was the day of the operation). Animals had been specifically selected that were of a friendly disposition, to make it easier to be able to identify any distress or requirements for additional analgesia, and to monitor the wound status, bowel and bladder functions and locomotion.

*Terminal physiological experiments*

Terminal physiological experiments were carried out between 15 and 18 (mostly 16) weeks following the lesion and are as described in more detail in Saywell et al. (2007). Animals were anesthetized with sodium pentobarbitone (initial dose 37.5 mg $kg^{-1}$ I.P., then I.V. as required), maintained under neuromuscular blockade with gallamine triethiodide (subsequent to surgery, repeated doses, 24 mg I.V., as required) and artificially ventilated via a tracheal cannula with oxygen-enriched air, so as to bring the end-tidal $CO_2$ fraction initially to about 4%. $CO_2$ was then added to the gas mixture to raise the end-tidal level to a value sufficient to give a brisk respiratory discharge in the mid-thoracic intercostal nerves (typically 6-7%). A low stroke volume and a high pump rate (53 $min^{-1}$) were employed so that events related to the central respiratory drive could be distinguished from those due to movement-related afferent input. Venous and arterial cannulae were inserted.

We aimed to use a (surgically adequate) level of anesthesia in the range light to moderately deep, as described by Kirkwood et al. (1982). Before neuromuscular blockade, a weak withdrawal reflex was elicited by noxious pinch applied to the forepaw, but not to the hind paw. When present, pinch-evoked changes in blood pressure (measured via a femoral arterial cannula), were absent or were small and of short duration. During neuromuscular blockade, anesthesia was assessed by continuous observations of the patterns of the respiratory discharges and blood pressure together with responses, if any, of both of these to a noxious pinch of the forepaw. Only minimal, transient responses (similar to those before neuromuscular blockade) were allowed before supplements (5 mg $kg^{-1}$) of pentobarbitone were administered. The responses to a noxious pinch always provided the formal criteria, but in practice the respiratory pattern, indicated by an external intercostal nerve discharge that was continuously monitored on a loudspeaker from the induction of neuromuscular blockade, always gave a premonitory indication. Any increase from the usual slow respiratory rate typical of barbiturate anesthesia (e.g. Fig. 2), led to such a test being carried out. The animal was supported, prone, by vertebral clamps, a clamp on the iliac crest and a plate screwed to the skull. The head was somewhat ventroflexed. Rectal temperature was maintained between 37° and 38°C by a thermostatically-controlled heating blanket. The bladder was emptied by manual compression at intervals. Systolic blood pressures were above 80 mmHg throughout. At the end of the experiment the animals were either killed with an overdose of anesthetic or were given a supplement of anesthetic and killed by perfusion for histology (see below).

Most of the data (120 acceptable motoneuron recordings, see below) come from 11 animals, where the primary aim was to measure the connections from EBSNs to motoneurons using spike-triggered averaging, but in the other 8 animals (32 acceptable motoneuron recordings) the primary aim was intracellular recording from interneurons (Meehan et al. 2003) and the motoneuron recordings were an inevitable by-product. These

152 animals were vagotomized and most also received a bilateral pneumothorax. Results did not differ between
153 these two groups, so they are considered together.
154
155 Nerves (see Fig. 1 of Saywell et al. 2007) were prepared for stimulation via platinum wire electrodes on
156 the left side of the segment immediately above the lesion, as described in detail by Saywell et al. (2007): (1) a
157 bundle of dorsal ramus nerves (Kirkwood *et al.* 1988); (2) the external intercostal nerve; (3) the most proximal
158 point on the internal intercostal nerve (in continuity, but arranged to be lifted away from the volume conductor
159 separately from the external intercostal nerve, so as to avoid stimulus spread); (4) the lateral branch of the
160 internal intercostal nerve; (5) the distal remainder of the internal intercostal nerve. These nerves were used for
161 antidromic identification of motoneurons, which therefore fell into 5 anatomical categories. The first two nerves
162 identified dorsal ramus (DR) motoneurons or external intercostal nerve (EI) motoneurons. Responses to the
163 lateral branch of the internal intercostal nerve identified external abdominal oblique (EO) motoneurons (Sears,
164 1964*a*), while motoneurons excited from the proximal electrodes on the internal intercostal nerve but not from
165 either of the more distal branches were identified as innervating the proximal part of internal intercostal or
166 intracostalis (Sears, 1964*a*) muscles (IIm motoneurons). Those identified from the distal remainder (Dist
167 motoneurons) innervated the distal part of internal intercostal muscle, other abdominal muscles, parasternal
168 intercostal muscle, or triangularis sterni (only at T7). For more detail of the muscles innervated and for
169 references, see Meehan et al. (2004) and Saywell et al. (2007). In the 8 experiments aimed primarily at
170 recording from interneurons, the lateral and distal internal intercostal nerve branches were not prepared and
171 the whole internal intercostal nerve (cut) was stimulated at the proximal site. In these animals, there were thus
172 only three categories, DR, EI and internal intercostal nerve (IIn). A combined category of EO, Dist, IIm, IIn
173 together (all internal intercostal nerve groups) was defined as IIN. The left external intercostal nerve of a rostral
174 segment (most often T6) was prepared for recording efferent discharges, which were used to define the timing
175 of central inspiration.
176 A thoracic laminectomy was made, the dura opened and small patches of pia removed from the dorsal
177 columns of the segment above the lesion, to be used for motoneuron recording. Stimulating electrodes, one
178 pair on each side of the cord were inserted into the left spinal cord 1-2 segments below the lesion as in
179 Kirkwood et al. (1988), together with another pair on the left side 1-2 mm rostral to the rostral edge of the scar
180 tissue overlying the lesion, and a shaped pressure plate lightly applied to the cord dorsum of the segment
181 above the lesion, to aid mechanical stability. The laminectomy and nerves were submerged in a single paraffin
182 oil pool constructed from skin flaps. In 16 of the animals, an occipital craniotomy was made, the dura opened
183 and a small patch of pia removed from the right side of the medulla.
184
185 *Recording procedures.*
186 The activities of EBSNs were recorded extracellularly in the right caudal medulla via glass
187 microelectrodes (broken back to a tip diameter of 3.0 – 3.2 μm and filled with 3M NaCl) introduced into the
188 medulla through a hole in a small pressure plate, and with conventional amplification. EBSNs within nucleus
189 retroambiguus, around 3 mm caudal to Obex, were identified by their expiratory firing patterns and by
190 antidromic identification from the stimulating electrodes on the left side rostral to the lesion (0.1 ms pulses).
191 They were also tested for antidromic activation from the electrodes caudal to the lesion and only accepted for

study if they failed to be activated at this site and were therefore deemed to have been axotomized in the lesion. This is justified by the high proportion (31/34) of EBSN axons that were antidromically activated at T9 and which could also be activated from T11 (Road et al. 2013). In four of the experiments, two recording electrodes were used, mounted on separate manipulators, so that two EBSNs could be used for STA with each motoneuron.

Intracellular recordings were made from motoneurons on the left side antidromically identified from stimulation of the peripheral nerves (see above), using glass microelectrodes inserted into the cord through the dorsal columns at an angle (tip lateral) of between 10 and 15 degrees. Recordings for most motoneurons were obtained with electrodes of external tip diameter 1.2 - 1.6 μm (resistance 2 - 5 MΩ) filled with 3M potassium acetate, although the electrodes used for 8 of the motoneurons had finer tips and were filled with 2% Neurobiotin (Vector laboratories) in 0.1M Tris buffer (pH 7.4) plus 0.5 M potassium acetate, as used for intracellular labelling of interneurons (Meehan et al. 2003).

Simultaneous recordings from the EBSNs, intracellular recordings from the motoneurons and the efferent discharges in the rostral external intercostal nerve were stored on magnetic tape and/or acquired for computer analysis (Spike2, CED, Cambridge, UK). Both a low-gain d.c. version and a high-gain, high-pass filtered (time-constant, 50 ms) version of the motoneuron membrane potential were included. The rostrocaudal positions of the motoneurons were noted with respect to the most rostral dorsal root on the left of the segment and fell within two regions approximately ± 0.5 mm of that rostral root or ± 0.5 mm of 5 mm more caudal, so as to be consistent with the control data from Saywell et al. (2007).

*Analysis*

Two basic comparisons were made with the control data. First, a description of the types and amplitudes of the central respiratory drive potentials (CRDPs, Sears, 1964b) as seen in the d.c. recording and, second, an analysis of the connectivity between the EBSNs and the motoneurons by spike-triggered averaging (STA), usually via the high-gain recording. For STA, the single unit nature of the EBSN recording was confirmed by the absence of very short intervals in an autocorrelation histogram (0.2 ms bins, examples in Fig. 4Aa,c). The lag to the first peak or the shoulder of the autocorrelation histogram was used to calculate an approximate modal firing frequency of the EBSN (Kirkwood 1995; Ford et al. 2000). Delays in the collision test and latencies in the STA measurements (Fig. 4) were all referred to the early rising phase of the (main) negative-going phase of the trigger spikes (Davies et al. 1985; Kirkwood, 1995). Orthodromic conduction times for the EBSNs were calculated from the collision test (routinely at 2x threshold, but see Results), as the critical delay minus 0.5 ms (Davies et al. 1985, verified by Kirkwood, 1995) and conduction velocities were calculated from these values together with distances from the medulla to the stimulating electrodes. These distances were calculated from a table of values related to the weight of the animal and derived from the animals used by Davies et al. (1985*a*) and Kirkwood (1995).The EBSN conduction time to the appropriate rostral or caudal part of the segment, the 'axonal time' (Davies et al. 1985; Kirkwood 1995), was calculated as the orthodromic conduction time to the stimulating electrodes multiplied by the ratio of distances to the motoneuron site and to the stimulating electrodes.

For motoneurons that were firing spontaneously, trigger spikes near times of spontaneous motoneuron spikes were edited out of the records before analysis, so that such spikes could not affect the averages. An

essential criterion for an averaged waveform to be accepted as a synaptic potential was that of repeatability; the potential (independent of any judgement about synaptic linkage) had to be present with a similar time course at the same latency in each of three successive averaging epochs (Kirkwood & Sears, 1982). Conventional shape indices (Rall, 1967; Jack et al. 1971) were measured for synaptic potentials (Fig. 6*D*), rise-times from 10% to 90% amplitude and durations at 50% amplitude (half-widths).

*Histological procedures*

The histology relevant to these experiments consisted of reconstructions of the extent of the spinal lesions. Animals from the interneuron series were heparinized and perfused through the left ventricle with a saline rinse, followed by 4% paraformaldehyde in phosphate buffer (pH 7.4). Relevant segments of spinal cord were removed and stored in the same fixative. In the other animals, the segment of the spinal cord containing the lesion was removed and immersion fixed in 10% formol saline. After an appropriate interval, serial transverse sections though the whole rostrocaudal extent of the lesions were cut and mounted, either wax-embedded, 15 μm, stained with cresyl violet and luxol fast blue, or frozen, 50 μm (after cryoprotection in sucrose), and stained with neutral red. Outlines of the sections through the lesion were traced via a drawing tube, to reconstruct the maximum extent of the lesion (not necessarily all from one section). Dark field illumination was included in this process, being particularly helpful at revealing small areas of myelination, indicating spared portions of fiber tracts (Fig. 1B).

Mean values are quoted as ± S.D. In statistical tests, $P < 0.05$ was taken as significant.

--- Fig. 1 near here ---

**RESULTS**

*Lesions*

The intended lesion was a complete section of all the white matter on the left side, except for the dorsal columns. However, as in Ford et al. (2000), only 4 of the lesions were complete (e.g. Fig. 1A). In the others some fibers were spared laterally and/or medially, within stereotyped locations in the spinal cord sections, probably determined by the shape of the scalpel blade and/or the spinal canal (Fig. 1B,C). Lesions were therefore rated separately for the lateral and medial locations, according to the scheme used by Ford et al. (2000) and as indicated in Fig. 1D. Larger lesions were assigned higher numbers, medially M1 to M4, laterally L0 to L4, where a complete lesion was rated L4/M4. Lesions complete medially and also extending to the right side (4 instances) were rated M5. Laterally, the majority of the lesions (12/19) were rated L4, the remainder L3. Medially, both the modal (7 instances) and the median ratings were M3, the mean was M3.16. As a group, the lesions were therefore very similar to the 16 week group of Ford et al. (2007) for their lateral extent, but were rather more complete medially. It was important that the ventral roots of the segment above the lesion were not damaged, to avoid the possibility of damaged axons re-innervating different muscles and making antidromic identification misleading. All spinal cords were carefully examined prior to cutting sections. Although the connective tissue scar was usually close to the

extradural ventral root, it never included it nor adhered to it, so we believe these roots were indeed undamaged.

*Motoneuron recordings*

Recordings were only acceptable if they had a baseline membrane potential, $V_m \leq -40$ mV. This was usually measured, as in Saywell et al. (2007), at the start of expiration, on the basis of this being the time in the respiratory cycle where the synaptic excitation or inhibition was likely to be least. However, since in many of the cells in the current experiments we found exaggerated post-inspiratory components in the CRDPs, in these cells $V_m$ was measured in late expiration. Values of $V_m$ varied between -40 and -81 mV (mean 54.7 ± 10.2 mV, n = 152).

--- Fig. 2 near here ---

*CRDPs*

Nearly all motoneurons (139/152) demonstrated CRDPs, which were characterized as in Saywell et al. (2007) as: (1) expiratory, with a ramp of excitation during expiration and a ramp of hyperpolarization during inspiration (presumed inhibition, as in Sears, 1964b), or (2) inspiratory, with a ramp of excitation during inspiration, or (3) expiratory decrementing ($E_{dec}$), with a depolarization greatest in early expiration, and a minimum (often with the appearance of an inhibitory phase) during inspiration (Fig. 2D,E). As mentioned above, the post-inspiratory component of inspiratory neurons was often exaggerated in the lesioned spinal cords, as were the post-inspiratory discharges of the external intercostal nerve recorded in a more rostral segment (Fig. 2D). In the control recordings from this category, as in other published data from inspiratory intercostal or phrenic motoneurons, the post-inspiratory depolarization most often had an amplitude of only a fraction of the size of the inspiratory depolarization, but in the lesioned spinal cords it was often large, sometimes being larger than that in inspiration. One might think that therefore these motoneurons should be classified as $E_{dec}$ instead of inspiratory. However the distinction we wish to make is that these inspiratory CRDPs showed a depolarizing ramp during inspiration (e.g. Fig. 2C), whereas those we have classified as $E_{dec}$ usually showed a hyperpolarization in inspiration (e.g. Fig. 2E). Moreover, the post-inspiratory component in the inspiratory neurons often varied in amplitude with time during a recording, sometimes in parallel with variation of the post-inspiratory component in the nerve discharges, while the inspiratory component stayed more-or-less constant. When we measured the amplitudes of these components we used a period in the recording when the cell was apparently in the best condition, usually near the start of the recording (Figs. 2D and E come from such periods). This also often was a time when the post-inspiratory component was largest. This component, in both the CRDP and the external intercostal nerve discharge frequently faded with time into a recording. This may have represented a general reduction of excitability after the nerve stimuli used during the antidromic identification procedures had been switched off, but by no means entirely: this level of excitability also appeared to wax and wane independently of any applied stimulation. A cycle-by-cycle variability in the post-inspiratory component was also relatively common, in either the external intercostal nerve discharge or in the CRDPs, but that in Fig. 2 D is an

extreme example. There were also a further 5 motoneurons with CRDPs that did not fit into the previous categories (see legend in Table 1: “other”), all of relatively low amplitude.

For all motoneurons, the measurements on the CRDPs included the overall peak-to-peak amplitude. For expiratory CRDPs, we also measured the expiratory ramp amplitude, as in Saywell et al. (2007) and, for inspiratory CRDPs, the maximum depolarization at the end of inspiration and that during post-inspiration, both referenced to the most hyperpolarized value, usually at end expiration. These latter measurements for the inspiratory CRDPs were different from those used by Saywell et al. (2007), so the CRDPs from that study were re-measured according to the new criteria, so that they could be directly compared. All the CRDP measurements, from both studies, were recorded to the nearest 0.5 mV

--- Table 1 near here ---

Table 1 lists the numbers and amplitudes of the different types of CRDP according to the groups of motoneurons identified by antidromic excitation from the different nerves and compares these with values from the control group from the experiments of Saywell et al. (2007). A few more motoneurons than were listed in the earlier study are now included in this group (those not used then for STA measurements). The group of motoneurons from the lesioned spinal cords also includes some not used for STA. A broadly similar sample of motoneurons from the different nerves is present for the two groups, with the one exception that for the lesion group there was a lower proportion of those in the IIn category, as compared to those in the Dist, EO and IIm categories. This reflects only that there was a lower proportion of animals in this study where the two branches of the internal intercostal nerve were not separately stimulated.

The distribution of CRDPs was broadly similar in the lesioned spinal cords to that in the controls. IIN motoneurons (i.e. IIn, EO or Dist) most often showed expiratory CRDPs, while inspiratory CRDPs were found most commonly in EI motoneurons or in Dist motoneurons. As previously, DR motoneurons showed a variety of CRDP types. However one clear difference was found: the proportion of CRDPs classified as $E_{dec}$ was clearly higher for the lesion than for the control groups. This was apparent across all categories of motoneurons and the difference overall (32/152 *vs.* 13/146) was significant ($\chi^2$, $p < 0.001$).

Given the starting point of this investigation, the observation of an increase in the physiologically measured EBSN projections in the segment above a lesion (Ford et al. 2000), the distribution of ramp amplitudes for expiratory motoneurons was of obvious interest. The mean amplitude was larger for the lesion group than for the controls (2.4 *vs.* 1.8 mV, medians 1.5 *vs.* 1.0 mV), but the difference was not significant (Mann-Whitney $p = 0.095$, one- tailed). The plasticity described by Ford et al. (2000) was detected only in the caudal half of the segment, so we also looked for a difference in the expiratory ramp amplitudes specifically for the caudally located groups of motoneurons. Again, the mean amplitude was slightly larger for the lesion than for the control group (2.2 *vs.* 1.8 mV, median 1.75 *vs.* 1.0 mV, n =29, n = 32 respectively) but again not significantly so (Mann-Whitney, $p = 0.38$ ).

--- Fig. 3 near here ---

An additional clear difference between lesion and control groups was found within the inspiratory CRDPs. As already mentioned, the post-inspiratory component was often exaggerated compared to normal. A quantification of this is shown in Fig. 3, where the post-Inspiratory amplitude is plotted against the inspiratory amplitude for each inspiratory CRDP of the two populations. Note that there were several examples in the lesion group like that in Fig. 2C, where the post inspiratory amplitude was larger than the inspiratory amplitude (points above the line of equality in Fig 3B). We measured the ratio of these two parameters for each inspiratory CRDP, and the difference was highly significant between the lesion and control groups (medians 0.57 and 0.19 respectively, Mann Whitney, $p < 0.0001$).

*EBSNs*

The discharges of 31 EBSNs were recorded and used for STA. The firing patterns of the EBSNs were similar to those in unlesioned animals, incrementing ramps of firing frequency, generally restricted to phase 2 expiration (Richter, 1982). Moreover, quantitative measures, the mean conduction velocity ( 57.1 ± 13.0 m $s^{-1}$) and the mean modal firing rate ( 75.5 ± 46.1 imp $s^{-1}$) were also similar to those measured for unlesioned animals in this laboratory. Thus, as in Ford et al (2000), we have no evidence that the physiological properties of the EBSNs in this group axotomized at T8-T10 were different from those previously reported from this laboratory (Kirkwood, 1995; Saywell et al. 2007; also see Sasaki et al. 1994), and we assume that the sample here is similar.

*STA*

Averages were constructed from the recordings of the above 31 EBSNs and 134 motoneurons, giving 180 EBSN-motoneuron pairs from 15 animals (1 – 16 motoneurons per EBSN). Each average involved more than about 1000 EBSN trigger spikes (range 926 to 60630 spikes, median 6289 spikes). Comparable figures from the control group were 957 to 22642 spikes, median 5233 spikes (n = 170). As in Saywell et al. (2007), averages that showed peak-to-peak noise > 10 μV (excluding slow drifts) were rejected. This excluded 18 averages (10 %). Comparable figures from the control group were 9 averages (5.3 %). Synchrony potentials, characterized by slow rising phases, usually starting earlier than the axonal time (Saywell et al. 2007) were detected in a few motoneurons. Of these 4 were large enough (amplitudes 17 to 33 μV) and had sufficiently fast rising phases to have obscured possible EPSPs of 10 μV or more in amplitude, which led to the elimination of these averages (2.2 %). The equivalent figure from the control group was 7 averages (3.9 %).

--- Fig. 4 near here ---

EPSPs were detected in 42 of the remaining 158 averages (Fig. 4), ranging in amplitude from 4 to 204 μV. In 12 of these averages, synchrony potentials were also detected (verified by repeatability), but were either small or slowly-rising enough not to hide a 10 μV EPSP, sometimes appearing as a clearly separate, slowly-rising “foot” preceding the EPSP (e.g. Fig. 4Ba). The EPSPs were distributed as indicated in Table 2, which also compares their distribution with those from the control experiments. The table is arranged similarly to Table 2 in Saywell et al. (2007), except that, because of the prominence of $E_{dec}$ CRDPs in the present data, this

category is now listed separately. Other minor numerical changes may be noticed as compared to the previous table. These result from our re-checking the control data and recalculating where required. Control and lesion populations (compare italics *vs.* bold in each category) were generally similar with regard to mean EPSP amplitudes. The apparently large differences in some of the smaller subgroups are to be expected, given the small numbers and the very wide ranges of amplitudes. There seemed to be consistent differences between the lesion and control groups in the proportions of the connections, these being generally lower in the lesion groups, but none of these differences were significant ($\chi^2$, $p > 0.05$). The difference for the one category where the lesion group showed a higher proportion of connections (motoneurons with $E_{dec}$ CRDPs) was also not significant (Fisher exact test, $p = 0.08$)

--- Table 2 near here ---

Given the starting point of this study (Saywell et al. 2007), we were particularly interested in possible increased connections in the caudal half of the segment for the lesion group. The “effective mean”, which shows the mean amplitude, including all tested motoneurons, (non-connections being counted as zero amplitude), should be the most appropriate measure to indicate increased connections. Clearly, no such increase was seen (Table 2D).

--- Fig. 5 near here ---

*Relation between EPSPs and CRDPs*

Even without the occurrence of a detectable increase in the overall connectivity with motoneurons, more subtle changes might be seen in the distributions of the connections within that pool. We have therefore investigated the variation in the distribution of EPSP amplitudes to motoneurons with different strengths of expiratory input. In Saywell et al. (2007) a clear relationship was present, where the motoneurons having the larger expiratory ramps showed both larger and more frequent connections. Fig. 5 shows that this was also true for the lesion population, using the same borderlines for ramp amplitude as previously .In particular, the effective mean amplitude showed a steady increase across the groups of increasing ramp amplitude. Note that the higher connectivity apparent in the “non-expiratory” group (8/26 connections, effective mean 5.0 μV) as compared to the same group in Saywell et al. (2007), where there were only 2/24 connections, effective mean 0.8 μV, is entirely the result of the increased number of $E_{dec}$ motoneurons in the lesion group. Within the non-expiratory subgroup, the $E_{dec}$ motoneurons received all of the connections (8/19, effective mean, 6.8 μV).

*EPSP latencies and time courses*

Another way in which plasticity in the EBSN terminals might be revealed is in changes in the time parameters for the EPSPs, as a result of more-branched or finer collaterals than in the controls. To investigate this, we first plotted the latencies of the EPSPs against the calculated axonal time (Fig. 6A,B), as in Saywell et al. (2007) (cf. Road et al. 2013, de Almeida & Kirkwood 2013). For both rostral and caudal groups, the latencies show a clear relationship with the axonal time, thus distinguishing these EPSPs from synchrony potentials, where no relationship is apparent (Davies et al. 1985; Saywell et. al 2007). The values for latency are grouped

a little above the line of equality, but rather differently for the rostral and caudal groups, the former showing more scatter, with both more points on or close to the line of equality and more points further away. Fig. 6C shows this explicitly, where the distributions of the segmental delay (the difference between EPSP latency and axonal time) are plotted. The means of these two distributions (0.71 ± 0.56 ms, n = 24 for the rostral group and 0.94 ± 0.31 ms, n = 18, for caudal one) are close to values from the control group (0.69 ± 0.38 ms, n = 55) or to the various values for the different groups of focal synaptic potentials in Ford et al. (2000).

--- Fig. 6 near here ---

Despite this similarity in the means, the apparently different distributions for the rostral and caudal groups here is intriguing. First, from an expectation of more sprouting in the caudal area, then more variability for the caudal group than for the rostral one might be expected, the reverse of what is apparent in Fig. 6C. Second, our implicit assumption, following Saywell et al. (2007) is that the observed EPSPs represent monosynaptic connections. However, for the rostral group, some of the shortest segmental delays are rather too short even for a monosynaptic connection, and some of the later ones (up to nearly 2ms) would allow for a disynaptic connection. We will return to this issue in the Discussion, but with regard to the particularly short delays it should be noted that there were several EBSNs reported by Ford et al (2000), particularly in the 16 wk lesion groups, where axonal potentials were observed in the extracellular averages with latencies shorter than the calculated axonal times (by more than 0.2 ms). For estimating segmental delay for these units, Ford et al (2000) used the directly observed axonal times in place of axonal times calculated from the collision test. Here we saw very few axonal potentials, probably because our averages were all made at sites within the motor nuclei, whereas those for Ford et al. (2000) included sites beyond these, including in or very close to the white matter. A number of terminal potentials were seen here (e.g. Fig. 4Ba,c), some of these being at latencies shorter than the calculated axonal times (Fig 4Ba). Like axonal potentials they have time-courses that are too short to arise via pre-synaptic synchrony, so these are in themselves evidence for some overestimation of the axonal times, supporting this as a likely explanation for the shortest of the EPSP latencies (see Discussion). Fig. 4Bc illustrates a particular verification of this explanation. Here the collision interval, measured at 2 × threshold predicted an axonal time for the location of the motoneuron concerned of 2.73 ms. However it was noticed that when the stimulating current was increased above 2 × threshold, the collision interval (unusually) shortened considerably, by much more than the 0.1 or 0.2 ms, that is normally typical for these axons, reaching a relatively constant value at 5 - 10 × threshold. This value at 5 × threshold was therefore adopted in this case, on the assumption that the longer collision intervals arose from the axon being stimulated at sites on fine collaterals. The axonal time was then calculated as 1.53 ms. As can be seen in Fig. 4Bc, the EPSP here (recorded in the caudal part of the segment) then showed, in place of a too-short segmental delay, one that was unusually long, 0.98 ms, as did EPSPs from another 4 motoneurons excited by this EBSN (0.82 - 0.96 ms). Moreover this EPSP is preceded by a clear terminal potential about 0.5 ms earlier. If the value of 2.73 ms had been adopted for the axonal time, then this terminal potential would have occurred about 0.7 ms earlier than this, and the EPSP itself would also have shown an unusually short segmental delay (-0.2 ms).

With regard to the other possible problem, the EPSPs with rather long segmental delays, we have investigated the possibility that these might arise from disynaptic connections by separately indicating

examples with segmental delay ≥ 1.2 ms, (triangles) on a conventional shape-index plot (Jack et al. 1971), with a view that disynaptic EPSPs would be likely to have longer rise-times than those generated monosynaptically (Fig. 6D). The overall distribution of rise-time and half-width values here is very similar to that in Fig. 6 of Saywell et al. (2007), which itself is similar to others in the literature for monosynaptic single-axon EPSPs (for refs, see Saywell et al. (2007). There were 8 examples with long segmental delays, but only one of these EPSPs had an extreme value for 10-90 % rise-time (1.34 ms), and this value itself is still within typical normal ranges (e.g. Jack et al. 1971).

## DISCUSSION

We originally set out to look for changes in the connectivity of EBSNs in the segment above and ipsilateral to a spinal cord lesion for which previous experiments using extracellular recording had indicated increased EBSN terminal projections. We did not find any significant changes in EBSN connections to motoneurons that would correspond to the change in projections. However, we did observe a different form of plasticity, a change in the distribution of CRDP types in the motoneurons. We will deal first with this.

### *Plasticity in CRDPs*

Significant increases in the proportion of $E_{dec}$ CRDPs and in the amplitudes of the post-inspiratory components in the inspiratory CRDPs were seen, compared to the control experiments. These may represent separate phenomena, but the simplest explanation, given the apparently uniform increase in the occurrence of $E_{dec}$ CRDPs across all categories of motoneurons, is that, following the lesion, there was a general addition of a post-inspiratory excitatory component to any motoneuron, including those that were previously expiratory and those that were previously inspiratory. In previous recordings in both thoracic and lumbar motoneurons, $E_{dec}$ CRDPs appeared to include an inhibitory component during inspiration (Kirkwood et al. 2002; Ford & Kirkwood 2006; Saywell et al. 2007; Wienecke et al. 2015). This component may or may not also have been generally increased, but if it was, it would not appear to have been large in the inspiratory motoneurons, or their definition as inspiratory, by virtue of showing an inspiratory ramp would not apply.

The occurrence of this increased excitation in post-inspiration in the segment above a lateral lesion is not entirely new. It was seen by Kirkwood et al. (1984) in external intercostal nerve discharges (see their Fig. 2), but was not then separated from the tonic excitation that could occur throughout expiration, particularly in the context of similar activity in more caudal segments below the lesion. Tonic excitation was not observed in the external intercostal discharges in the present experiments. However, the recordings of these discharges here were made 2-3 segments rostral to the lesion rather than in the segment next to the lesion and also hypercapnia was used here throughout, rather than the hypocapnia which was used to reveal the tonic excitation by Kirkwood et al. (1984). The tonic excitation seen previously in external intercostal motoneurons was associated with large amplitude, synchronized synaptic noise and a respirator-phased stretch reflex excitation. Here, neither of these was obvious, though large amplitude synaptic noise, usually having the appearance of individual EPSPs or IPSPs was specifically noted in a number of motoneurons. Such noise was probably the reason why a relatively large proportion of STA averages (10%) were rejected because of high

base-line noise. In particular, large amplitude EPSPs could often be seen during post-inspiratory depolarizations. The small deflections of amplitude 2 - 4 mV during post-inspiration in Fig. 2B, D, which could be confused for miniature spikes when seen on the time scale used in the figure, were actually EPSPs, as was apparent when the recordings were examined on a faster time scale (Fig. 7).

--- Fig. 7 near here ---

The tonic excitation observed by Kirkwood et al. (1984) was interpreted as originating in interneurons, released by the lesions from descending controls. We suggest the same is likely to be the case here, though, in the absence of the synchronization and the stretch reflex, probably not the same interneurons. We suggest interneurons as the source, rather than an increased input from descending fibers, because $E_{dec}$ bulbospinal neurons have very rarely been seen (Miller et al. 1985; Ezure 1990; Boers et al. 2005; Ford & Kirkwood, 2006), and none were seen during this series. Nor did we see any appreciable post-inspiratory discharge in any of the EBSNs recorded here. Nevertheless we cannot totally exclude an increased $E_{dec}$ input from the medulla (for instance if there was a population of $E_{dec}$ bulbospinal neurons that were small and hard to record from and hence as yet unidentified).

As for the suggestion of a “release” phenomenon, rather than longer term plasticity, we can again only follow the logic of Kirkwood et al. (1984), where an increased post-inspiratory component of the external intercostal nerve discharges was recorded as early as 3 days post- lesion (Kirkwood et al. 1984, Fig. 2A). Here, only the one time point (16 weeks post lesion) was studied. One minor caveat must also be kept in mind when comparing the present results with those of Kirkwood et al. (1984), in that in the previous study, the ipsilateral dorsal columns were sectioned, whereas here they were generally spared.

The question can be asked as to whether the increased post-inspiratory components were part of a useful functional adaptation to the changed mechanical circumstances following the lesions. First, it should be noted that such mechanical changes are not as large as one might imagine. It is not the case that the previously balanced drive to adjacent intercostal spaces would have been lost; the situation here should have been the same as in the experiments of Kirkwood et al. (1984), where the respiratory output in the segments below the lesion was restored to near normal levels (albeit including a tonic component). In any case, if the increased post-inspiratory components did comprise a functional adaptation, such an adaptation should be considered as plasticity, not a reflex effect, since the mechanical circumstance during the experiments, with neuromuscular blockade and artificial ventilation should have been the same in the present experiments as in the controls. It can also be argued that if the adaptation is functional, it is likely that the function concerned is not respiratory, because the additional excitation seemed to be very general, to all classes of motoneuron, and not selective to one or other layer or region of the thorax. However, this argument cannot be conclusive, given our limited understanding of the functional synergies of the muscles concerned (see discussion in Ford et al. 2014).

The functional role of the post-inspiratory components of excitation in general nevertheless needs some consideration. Easton et al. (1999), argued against a commonly accepted view (Remmers & Bartlett, 1977) that this component had a specific respiratory role, that of slowing the early expiratory air flow, by pointing out that, in the awake dog, the component was much larger for the interosseous intercostals than for

the more important inspiratory muscles, the parasternal intercostals. Here, there was no apparent difference for the post-inspiratory to inspiratory ratio between the EI and the IIN motoneurons, for either the control or the lesion populations (Fig. 3). However, this does not mean that we are therefore arguing for a specific respiratory function. The great variability and apparent independence between the inspiratory and post-inspiratory components rather argues the reverse. One new clue as to a possible function for this component has come from recent analyses of the respiratory drive in hind limb motoneurons. This drive is most often of the $E_{dec}$ type (Ford & Kirkwood, 2006) and it now seems most likely, at least in the decerebrate, that this signal is transmitted via the central pattern generator for locomotion, allowing the locomotor drive to be synchronized to the respiratory one (Wienecke et al. 2015). In the medulla, from Richter (1982) onwards, post-inspiratory neurons have been assigned important roles in the generation of the normal respiratory pattern (e.g. Smith et al. 2007). These observations might suggest a more general role for post-inspiratory neurons in phase transitions, throughout the medulla and spinal cord, although what is seen in lumbar motoneurons, as here, is post-inspiratory excitation, whereas the role of these neurons in the medulla is believed to be inhibitory. Post-inspiratory interneurons are common in the thoracic segments (Kirkwood et al. 1988), including both excitatory and inhibitory types (Schmid et al. 1993), but, as pointed out by Saywell et al. (2007), the fact that they demonstrate this respiratory pattern in the anesthetized animal under hypercapnia may merely reflect a default behavior under this particular condition. In an awake animal, they could reflect whatever rhythmic drive is dominant at any one time. This view could be seen as a more general expression of the hypotheses put forward by Dutschman et al. (2014), where the rather particular non-respiratory role of post-inspiratory neurons in controlling the airway-defensive actions of the laryngeal adductor muscles were emphasised. In the conditions of the present experiments, we do not know why the drive from these inputs to thoracic motoneurons should be exaggerated. Perhaps it simply reflects their ubiquity.

Finally, one might consider whether the increase in post-inspiratory depolarization might represent a change in intrinsic motoneuron properties. We made no attempt to measure such properties, but one could note that the increased depolarization was seen both in $E_{dec}$ motoneurons, where it followed a presumed inhibition, and in inspiratory motoneurons, when it followed a depolarization. Moreover, for CRDPs such as that illustrated in Fig. 2D, where the large post-inspiratory depolarizations are strongly linked to similar behavior in the more rostral external intercostal nerve, it seems most likely that a strong synaptic excitation is involved, which is also consistent with the large individual EPSPs occurring at these times (Fig. 7).

*Absence of plasticity in the EBSN connections*

The distribution of EBSN EPSPs in the motoneurons of the segment above lesions was remarkably similar to that in the controls. This was despite the considerable deafferentation that was likely for the motoneurons and the severance of the EBSN axons in the lesions. The expectation from the plasticity in EBSN projections reported earlier (Ford et al. 2000) was that the connections might have become stronger. If anything they were found to be weaker, though not significantly so. The one category of connections that appeared stronger, though again not significantly so, that to the $E_{dec}$ motoneurons, would also probably not represent a real increase in connections to the motoneurons concerned, even if the change had been significant, since we cannot know how these motoneurons would have been defined before the lesions. For many of these (in the IIN category), their CRDPs could previously have shown small expiratory ramps, which would have needed the

addition of only a relatively small post-inspiratory depolarizing component to be converted to an $E_{dec}$ time course.

Of course, we do not know whether or not any of the connections were actually the same as before the lesions, or whether in the intervening 16 weeks a series of changes had occurred, ending up with connections in the same proportions and specificities as originally. This is why we looked carefully at the EPSP segmental delays. Whereas the variations in segmental delay do allow for a certain amount of sprouting (as was the case for the focal synaptic potentials in Ford et al. 2000), the changes here compared to the controls (Saywell et al. 2007, Fig. 7A) are not sufficient to conclude that this has taken place. There is a sufficient alternative explanation for the unusually short segmental delays, as explained under Results. Note that it may not only be that the antidromic activation in the collision test had occurred at sites on collaterals, but it could also be that the main axon conduction velocity may have itself been reduced in the few mm rostral to the lesion. For the segmental delays that are unusually long (up to nearly 2 ms), there is certainly time for a disynaptic connection, but note that in Ford et al. (2000), there was a similar tail in the distribution of segmental delays of focal synaptic potentials, supported by an equivalent distribution of terminal potentials. The terminal potentials have time courses too short to have been recorded over a disynaptic link. Moreover, in any population of single fiber EPSPs there are usually a few with abnormally long latencies, as a result of long or branched collaterals (e.g. Kirkwood, 1995, Fig. 9D) and/or by virtue of an origin in a dendritic location. Only when a clearly separate population of motoneurons with appropriately long segmental delays can be independently identified is it valid to conclude that a population of di- (or oligo-) synaptic connections exists (de Almeida & Kirkwood, 2013).

Overall, therefore, this study has emphasized the stability in the EBSN connections to motoneurons, despite the extended EBSN projections identified by Ford et al. (2000). However, at least two possibilities still exist for these. The first is connections to interneurons. Plentiful interneurons with expiratory activity are present in the thoracic spinal cord under the conditions of these experiments (Kirkwood et al. 1988) and their expiratory activity is almost certainly ultimately derived from EBSNs. Although such connections to interneurons have yet to be demonstrated, one could speculate that the (non-significant) increase in the expiratory ramp amplitude observed here was the result of increased oligosynaptic connections via local interneurons. The second possibility is that of possible connections to gamma motoneurons, which are not generally present in an intracellular sample. This possibility is presently under investigation by a re-analysis of the data of Ford & Kirkwood (1995), which consist of EBSN and efferent motoneuron discharges recorded in the same animals as used in Ford et al. (2000).

## REFERENCES

**Anissimova NP, Saywell SA, Ford TW, Kirkwood PA.** Dissociation between inspiratory and post-inspiratory components in the excitation of external intercostal motoneurones in the cat following lesions of the spinal cord. *Eur J Neurosci* 12: Suppl. 11, 333**,** 2000.

**Anissimova NP, Saywell SA, Ford TW, Kirkwood, PA.** Distributions of EPSPs from individual expiratory bulbospinal neurones in the normal and the chronically lesioned thoracic spinal cord. *XXXIV Int Congress Physiol Sci*: Abstr 1029, 2001

**Arvanian VL, Bowers WJ, Anderson A, Horner PJ, Federoff HJ, Mendell LM.** Combined delivery of neurotrophin-3 and NMDA receptors 2D subunit strengthens synaptic transmission in contused and staggered double hemisected spinal cord of neonatal rat. *Exp Neurol* 197: 347–352, 2006.

**Bareyre FM, Kerchensteiner M, Raineteau O, Mettenleiter TC Weinmann O, Schwab ME.** The injured spinal cord spontaneously forms a new intraspinal circuit in adult rats. *Nat Neurosci* 7: 269-277, 2004.

**Becker MI, Parker D.** Changes in functional properties and 5-HT modulation above and below a spinal transection in lamprey. Front Neural Circuits 8: 148. doi: 10.3389/fncir.2014.00148, 2015

**Boers J, Ford TW, Holstege G, Kirkwood PA.** Functional heterogeneity among neurons in the nucleus retroambiguus with lumbosacral projections in female cats. *J Neurophysiol* 94: 2617-2629, 2005.

**Conta AC, Steltzner DJ.** Differential vulnerability of propriospinal tract neurons to spinal cord contusion injury. *J Comp Neurol* 479: 347-359, 2004.

**Conta Steencken AC, Stelzner DJ.** Loss of propriospinal neurons after spinal contusion injury as assessed by retrograde labeling. *Neurosci* 170: 971-980 2010.

**Conta Steencken AC, Smirnov I, Stelzner DJ.** Cell survival or cell death: differential vulnerability of long descending and thoracic propriospinal neurons to low thoracic axotomy in the adult rat. *Neurosci* 194: 359-371, 2011.

**Courtine G, Song B, Roy RR, Zhong H, Herrmann JE, Ao Y, Qi J, EdgertonVR, Sofroniew MV.** Recovery of supraspinal control of stepping via indirect propriospinal relay connections after spinal cord injury. *Nature Med* 14: 69-74, 2008.

**Davies JGMcF, Kirkwood PA, Sears TA.** The detection of monosynaptic connexions from inspiratory bulbospinal neurones to inspiratory motoneurones in the cat. *J Physiol* 368: 33-62, 1985.

**de Almeida ATR, Kirkwood PA.** Specificity in monosynaptic and disynaptic bulbospinal connections to thoracic motoneurones in the rat. *J Physiol 591*: 4043-40634, 2013..

**Dutschmann M, Jones SE, Subramanian HH, Stanic D, Bautista TG.** The physiological significance of postinspiration in respiratory control. *Progr Brain Res* 212: 113-130, 2014.

**Easton PA, Hawes GH, Rothwell B, De Troyer A.** Postinspiratory activity of the parasternal and external intercostal muscles in awake canines. *J Appl Physiol* 87: 1097–1101, 1999.

**Ezure K.** Synaptic connections between medullary respiratory neurons and considerations on the genesis of respiratory rhythm. *Prog Neurobiol* 35: 429-450, 1990.

**Fawcett J.** Repair of spinal cord injuries: where are we, where are we going? *Spinal Cord* 40: 615-623, 2002.

**Flynn JR, Graham BA, Galea MP, Callister RJ.** The role of propriospinal interneurons in recovery from spinal cord injury. *Neuropharmacol* 60: 809-822, 2011.

**Ford TW, Kirkwood PA.** Connections of expiratory bulbospinal neurones in the anaesthetized cat before and after axotomy. *J Physiol* 487P:67-68P, 1995.

**Ford TW, Kirkwood PA.** Respiratory drive in hindlimb motoneurones of the anaesthetized female cat. *Brain Res Bull* 70: 450-456, 2006.

**Ford TW, Meehan CF, Kirkwood PA.** Absence of synergy for monosynaptic group I inputs between abdominal and Internal intercostal motoneurons. *J Neurophysiol* 112:1159-1168, 2014.

**Ford TW, Vaughan CW, Kirkwood PA.** Changes in the distribution of synaptic potentials from bulbospinal neurones following axotomy in cat thoracic spinal cord. *J Physiol* 524:163-178, 2000.

**Jack JJB, Miller S, Porter R, Redman SJ.** The time course of minimal excitatory post-synaptic potentials evoked in spinal motoneurones by group Ia afferent fibres. *J Physiol* 215: 353-380, 1971.

**Kirkwood PA.** Synaptic excitation in the thoracic spinal cord from expiratory bulbospinal neurones in the cat. *J Physiol* 484: 201-225, 1995.

**Kirkwood P, Enríquez Denton M, Wienecke J, Nielsen JB, Hultborn H.** Physiological roles for persistent inward currents in motoneurones: insights from the central respiratory drive. *Biocybernet Biomed Eng* 38: 31-38, 2005

**Kirkwood PA, Lawton M, Ford TW.** Plateau potentials in hindlimb motoneurones of female cats under anaesthesia. *Exp Brain Res* 146: 399-403, 2002.
.

**Kirkwood PA, Munson JB, Sears TA, Westgaard RH.** Respiratory interneurones in the thoracic spinal cord of the cat. *J Physiol* 395: 161-192, 1988.

**Kirkwood PA, Sears TA.** Excitatory post-synaptic potentials from single muscle spindle afferents in external intercostal motoneurones in the cat. *J Physiol* 322: 287-314, 1982.

**Kirkwood PA, Sears TA, Westgaard RH.** Restoration of function in external intercostal motoneurones of the cat following partial central deafferentation. *J Physiol* 350: 225–251, 1984.

**Kirkwood PA, Schmid K, Sears TA.** Functional identities of thoracic respiratory interneurones in the cat. *J Physiol* 461: 667-687, 1993.

**Kirkwood PA, Sears TA, Tuck DL, Westgaard RH.** Variations in the time course of the synchronization of intercostal motoneurones in the cat. *J Physiol* 327: 105-135, 1982.

**Meehan CF, Ford TW, Kirkwood PA**. Dendritic and possible axonal sprouting by thoracic interneurons in the lesioned spinal cord. Program No. 498.6. *2003 Abstract Viewer/Itinerary Planner.* Washington, DC: Society for Neuroscience. Online, 2003.

**Meehan CF, Ford TW, Road JD, Donga R, Saywell SA, Anissimova NP, Kirkwood PA.** Rostrocaudal distribution of motoneurones and variation in ventral horn area within a segment of the feline thoracic spinal cord. *J Comp Neurol* 472: 281-291, 2004.

**Miller AD, Ezure K, Suzuki I.** Control of abdominal muscles by brain stem respiratory neurons in the cat, *J Neurophysiol* 54: 155–167. 1985.

**Rall W.** Distinguishing theoretical synaptic potentials computed for different soma-dendritic distributions of synaptic input. *J Neurophysiol* 30: 1138-1168, 1967.

**Remmers JE, Bartlett D.** Reflex control of expiratory airflow and duration. *J Appl Physiol* 42: 80–87, 1977.

**Richter DW.** Generation and maintenance of the respiratory rhythm. *J Exp Biol* 100: 93–107, 1982.

**Road JD, Ford TW, Kirkwood PA.** Connections between expiratory bulbospinal neurons and expiratory motoneurons in thoracic and upper lumbar segments of the spinal cord. *J Neurophysiol* 109: 1837-1851, 2013.

**Sasaki S, Uchino H, Uchino Y.** Axon branching of medullary expiratory neurons in the lumbar and sacral spinal cord of the cat. *Brain Res* 648: 229-238, 1994.

**Saywell SA, Anissimova NP, Ford TW, Meehan CF, Kirkwood PA.** The respiratory drive to thoracic motoneurones in the cat and its relation to the connections from expiratory bulbospinal neurones. *J Physiol* 579: 765-782, 2007.

**Saywell SA, Ford TW, Meehan CF, Todd AJ, Kirkwood PA.** Electrical and morphological characterization of propriospinal interneurons in the thoracic spinal cord. *J Neurophysiol* 105: 806–826, 2011.

**Schmid K, Kirkwood PA, Munson JB, Shen E, Sears TA.** Contralateral projections of thoracic respiratory interneurones in the cat. *J Physiol* 461: 647-665, 1993.

**Sears TA.** The fibre calibre spectra of sensory and motor fibres in the intercostal nerves of the cat. *J Physio*l 172: 150-160, 1964a.

**Sears TA**. The slow potentials of thoracic respiratory motoneurones and their relation to breathing. *J Physiol* 175: 404-424, 1964b.

**Smith JC, Abdala AP, Koizumi H, Rybak IA, Paton JF.** Spatial and functional architecture of the mammalian brain stem respiratory network: a hierarchy of three oscillatory mechanisms. *J Neurophysiol* 98: 3370 –3387, 2007.

**Wienecke J, Enríquez Denton M, Stecina K, Kirkwood PA, Hultborn H.** Modulation of spontaneous locomotor and respiratory drives to hindlimb motoneurons temporally related to sympathetic drives as revealed by Mayer waves. *Front. Neural Circuits* 9:1. doi: 10.3389/fncir.2015.00001, 2015.

## ACKOWLEDGEMENTS

Thanks are due to the late SA Saywell for assistance in some experiments, to K Sunner for histological assistance and to the animal care staff of the Institute of Neurology for their dedicated attention to the operated animals. Present addresses: TWF, University of Nottingham School of Health Sciences, Queen's Medical Centre, Nottingham NG7 2HA, UK; CFM, Department of Neuroscience and Pharmacology, 33.3 Panum Institute, Blegdamsvej 3, 2200 København N, Denmark.

## GRANTS

The work was funded by the International Spinal Research Trust. CFM held a Medical Research Council (MRC) studentship.

## AUTHOR CONTRIBUTIONS

Author contributions: TWF, NPA, CFM, PAK performed experiments; TWF, NPA, CFM, PAK interpreted results of experiments; TWF, CFM, PAK edited and revised manuscript; TWF, NPA, CFM, PAK saw the final version of manuscript; TWF, CFM, PAK approved the final version of manuscript; NPA gave prior approval to the conclusions in the manuscript. TWF, NPA, PAK conception and design of research, TWF, NPA, PAK analyzed data; PAK prepared figures; PAK drafted manuscript.

## FIGURE LEGENDS

**Figure 1. Lesions and their classification.** Transverse sections of the spinal cord are shown. A, an example of a lesion which was close to ideal. The black area indicates an absence of neurons or intact myelinated fibers. The small clear area extending laterally to the left from the central canal was a small cyst. B, the use of darkfield illumination to help show up small areas of surviving white matter (arrow). C, the reconstruction of the lesion illustrated in B (arrow as in B). D, schematic of the classification of lesion borders, laterally (L1 – L3) and medially (M0 to M3). Lesions which were complete laterally or complete to the midline medially were rated L4 or M4 respectively (see text for more detail). The lesion in A was rated L4/M4, that in B,C was rated L3/M2.

**Figure 2. Examples of CRDPs of different types, from various categories of motoneuron.** A, expiratory CRDP, IIm motoneuron; B, inspiratory CRDP, EI motoneuron; C, inspiratory CRDP, with a post-inspiratory depolarization a little larger than the inspiratory component, EI motoneuron; D, expiratory decrementing ($E_{dec}$) CRDP, IIm motoneuron; E, $E_{dec}$ CRDP, EO motoneuron. In each panel the intracellular recording is shown (bottom trace) with the external intercostal nerve discharge from a more rostral segment in the trace above. In A, simultaneous recordings from two EBSNs are also included, with their instantaneous firing frequencies shown above each EBSN recording.

**Figure 3. Comparison between the post-inspiratory components of inspiratory CRDPs between cells in lesioned and control spinal cords.** The post-inspiratory amplitude is plotted against the inspiratory amplitude for each CRDP in the three categories of anatomical motoneuron identification, as indicated by the different symbols. For each of the plots, the line is the line of identity.

**Figure 4. Examples of STA EPSPs recorded in various categories of motoneuron.** A, full analysis for the motoneuron illustrated in Fig. 2A (expiratory IIm): a,c, auto-correlation histograms from the upper and lower EBSNs respectively in Fig. 2A; b,d, EPSPs averaged, respectively, from those two EBSNs. B, STA EPSPs averaged from other motoneurons: a, $E_{dec}$ Dist motoneuron; b, inspiratory DR motoneuron; c,

828 inspiratory EI motoneuron (the same as in Fig. 2C), as indicated. The averaged EBSN trigger spike is
829 shown below each EPSP and the calculated axonal time (see Methods) is indicated by the arrow. Numbers
830 of sweeps: Aa, 14,416; Ab, 20,472; Ba, 10,046; Bb, 21,582;Bc, 11,378.
831
832 **Figure 5. Summarized EPSP and CRDP parameters for IIN motoneurons.** EPSP amplitudes are
833 grouped according to CRDP amplitude and displayed graphically (note the log scale). For the definition of
834 effective mean amplitude see text and Table 2.
835
836 **Figure 6. Timing characteristics of the EPSPs.** A, B, EPSP latencies plotted against the axonal time for
837 the rostral and caudal groups of recordings respectively. The lines are the lines of identity. C, Distributions
838 of segmental delay (difference between EPSP latency and axonal time) for the same two groups. D,
839 conventional shape indices for the EPSPs. Open symbols, rostral group; filled symbols, caudal group;
840 circles, EPSPs with segmental delays < 1.2 ms; triangles, EPSPs with segmental delays ≥ 1.2 ms.
841
842 **Figure 7. Synaptic noise in post-inspiration.** Expanded traces from two of the recordings in Fig. 2, to
843 illustrate the synaptic noise present in post-inspiration (right panels). For comparison, similar extracts from
844 the preceding inspiration are included in the left panels. A, from the inspiratory EI motoneuron in Fig. 2B
845 (second respiratory cycle). B, from the $E_{dec}$ IIm motoneuron in Fig. 2D (first respiratory cycle). The upper
846 trace in each panel is the external intercostal nerve recording. The 3 motoneuron spikes in A during
847 inspiration and the one in B during post-inspiration are truncated. The time calibration applies to all panels.

| Motoneuron Group | | Dist | | EO | | IIm | | IIn | | EI | | DR | | Total | |
|---|---|---|---|---|---|---|---|---|---|---|---|---|---|---|---|
| CRDP Type | | *Control* | **Lesion** | *Control* | **Lesion** | *Control* | **Lesion** | *Control* | **Lesion** | *Control* | **Lesion** | *Control* | **Lesion** | *Control* | **Lesion** |
| **Insp** | n | *8* | **5** | - | - | - | - | *10* | **4** | *17* | **17** | *16* | **9** | *51* | **35** |
| | range (mV) | *0.5-13* | **2-13** | - | - | - | - | *3.5-19* | **1-8** | *1-17* | **2-12** | *0.5-4.5* | **0.5-7** | *0.5-19* | **0.5-13** |
| | mean (mV) | *4.3* | **7.1** | - | - | - | - | *10.1* | **4.4** | *7.3* | **5.8** | *2.2* | **2.3** | *5.8* | **5.0** |
| | S.D. | *4.3* | **4.9** | - | - | - | - | *5.7* | **3.1** | *4.4* | **2.6** | *1.1* | **1.8** | *5.0* | **3.3** |
| **Exp** | n | *23* | **26** | *16* | **16** | *11* | **10** | *22* | **10** | - | **1** | *1* | **4** | *73* | **67** |
| | range (mV) | *0.5-11.5* | **1-12** | *1-11.5* | **1-14** | *1.5-15.5* | **2.5-16** | *1.5-10.5* | **2-12** | - | **2** | *1* | **1-3.5** | *0.5-15.5* | **1-16** |
| | mean (mV) | *4.5* | **4.2** | *4.3* | **5.0** | *4.9* | **7.3** | *4.7* | **6.1** | - | - | - | **2.5** | *4.7* | **5.0** |
| | S.D. | *2.9* | **3.0** | *3.0* | **4.0** | *2.7* | **3.7** | *2.6* | **3.2** | - | - | - | **1.1** | *3.1* | **3.6** |
| | **(ramps)** | | | | | | | | | | | | | | |
| | range (mV) | *0-6* | **0-7** | *0-5* | **0-8.5** | *0-6* | **0-8.5** | *0-5* | **1-10** | - | **0.5** | *0* | **0-1.5** | *0-6* | **0-10** |
| | mean (mV) | *2.0* | **2.1** | *1.5* | **2.3** | *2.1* | **3.1** | *1.6* | **3.5** | - | - | - | **0.5** | *1.8* | **2.4** |
| | S.D. | *1.6* | **1.9** | *1.3* | **2.9** | *1.9* | **2.2** | *1.6* | **3.0** | - | - | - | **0.6** | *1.6* | **2.5** |
| **$E_{dec}$** | n | *2* | **7** | - | **3** | - | **2** | *2* | **2** | *4* | **9** | *5* | **9** | *13* | **32** ** |
| | range (mV) | *2.5,6* | **1.5-3.5** | - | **2-5.5** | - | **3, 4.5** | *2, 3* | **2, 3.5** | *0.5-4* | **1-8** | *0.5-3* | **0.5-6** | *0.5-6* | **0.5-8** |
| | mean (mV) | *4.2* | **2.2** | - | **4.2** | - | **3.8** | *2.5* | **2.8** | *2.1* | **3.7** | *1.9* | **1.8** | *2.4* | **2.8** |
| | S.D. | - | **0.6** | - | **1.5** | - | - | - | - | *1.4* | **2.4** | *0.9* | **1.7** | *1.4* | **1.9** |
| **Other** | n | - | - | - | **1** | - | - | - | - | - | **2** | *1* | **2** | *1* | **5** |
| | range (mV) | - | - | - | **3** | - | - | - | - | - | **3.5, 4** | *2.5* | **0.5, 0.5** | *2.5* | **0.5-4** |
| | mean (mV) | - | - | - | - | - | - | - | - | - | - | - | **0.5** | - | **2.3** |
| | SD. | - | - | - | - | - | - | - | - | - | - | - | - | - | **1.5** |
| **No CRDP** | n | *1* | **2** | - | **2** | *1* | - | *2* | - | *2* | **1** | *2* | **8** | *8* | **13** |
| **Total (with CRDP)** | | | | | | | | | | | | | | | |
| | n | *33* | **38** | *16* | **20** | *11* | **12** | *34* | **16** | *21* | **29** | *23* | **24** | *138* | **139** |
| | range (mV) | *0.5-13* | **1-13** | *1-11.5* | **1-14** | *1.5-15.5* | **2.5-16** | *1.5-19* | **1-12** | *0.5-17* | **0.5-12** | *0.5-4.5* | **0.5-7** | *0.5-19* | **0.5-16** |
| | mean (mV) | *4.4* | **4.2** | *4.3* | **4.8** | *4.9* | **6.7** | *6.1* | **6.6** | *6.4* | **4.6** | *2.1* | **2.1** | *4.9* | **4.3** |
| | S.D. | *3.3* | **3.4** | *3.0* | **3.7** | *2.7* | **3.7** | *4.6* | **5.7** | *4.5* | **2.9** | *1.0* | **1.7** | *3.9* | **3.4** |

**Table 1. Numbers and amplitudes of CRDPs of each type for each motoneuron group.** Data from current experiments (bold) are compared with control data, from Saywell et al. (2007) (italics). The CRDP category "other" includes: (controls) 1 expiratory-inspiratory; (lesion) 3 inspiratory decrementing (2 EI, 1 DR) and 2 multiphasic (1 EO, 1 DR). The only notable difference between the lesion and control populations (see text) is in the proportion of $E_{dec}$ CRDPs (**).

**Table 2. Number and amplitudes of EPSPs in motoneurons of different groups.**

| | Connectivity | | Amplitude (μV) | | | |
|---|---|---|---|---|---|---|
| | | | Mean | | Effective mean | |
| | *Control* | **Lesion** | *Control* | **Lesion** | *Control* | **Lesion** |
| **A. IIN Motoneurons with expiratory CRDPs** | | | | | | |
| Dist | *16/26 (62%)* | **10/31 (32%)** | *22.2* | **35.0** | *13.6* | **11.3** |
| EO | *12/20 (60%)* | **6/16 (38%)** | *41.9* | **20.1** | *25.1* | **7.5** |
| IIm | *8/12 (75%)* | **7/13 (54%)** | *39.8* | **87.5** | *31.9* | **47.1** |
| IIn | *8/22 (36%)* | **3/5 (60%)** | *79.3* | **24.9** | *28.8* | **14.9** |
| Total IIN exp. | *44/80 (55%)* | **26/65 (40%)** | *41.1* | **44.5** | *21.1* | **17.8** |
| **B. Motoneurons with inspiratory CRDPs** | | | | | | |
| Dist | *1/11* | **0/5** | *15.0* | - | *1.4* | - |
| IIn | *2/8 (25%)* | - | *9.3* | - | 2.3 | - |
| EI | *2/16 (13%)* | **3/20 (15%)** | *38.2* | **39.2** | *5.1* | **5.9** |
| DR | *3/14 (23%)* | **1/10 (10%)** | *19.7* | **16.7** | *4.2* | **1.7** |
| Total insp. | *8/49 (16%)* | 4/35 (11%) | *20.1* | **33.5** | *3.3* | **3.8** |
| **C. Motoneurons with $E_{dec}$ CRDPs** | | | | | | |
| Dist | *0/1* | **6/10 (60%)** | - | **14.7** | - | **8.8** |
| EO | - | **1/4 (25%)** | - | **33.9** | - | **8.5** |
| IIm | - | **1/4 (25%)** | - | **7.5** | - | **1.9** |
| IIn | *0/2* | **0/1** | - | - | - | - |
| EI | *0/5* | **2/9 (22%)** | - | **17.3** | - | **8.8** |
| DR | *1/5 (20%)* | **2/11 (18%)** | *34.0* | **14.4** | *6.8* | **2.6** |
| Total $E_{dec}$ | *1/13 (8%)* | 12/39 (31%) | *34.0* | **33.6** | *2.6* | **4.9** |
| **D. Motoneurons with other CRDPs and no CRDP** | | | | | | |
| Dist | *0/1* | **0/1** | - | - | - | - |
| EO | - | **0/1** | - | - | - | - |
| IIm | *0/1* | - | - | - | - | - |
| IIn | *0/2* | - | - | - | - | - |
| EI | *1/2 (50%)* | **0/4** | *65.0* | - | *32.5* | - |
| DR | *1/6 (17%)* | **0/13** | *6.0* | - | *1.0* | - |
| Total other | *2/12 (17%)* | **0/19** | *35.5* | - | *5.9* | - |
| **Grand total** | *55/154 (36%)* | **42/158 (27%)** | *37.7* | **35.3** | *13.5* | **9.4** |
| **E. Rostral vs. caudal parts of the segment** | | | | | | |
| Rostr IIn exp | *27/52 (52%)* | **16/34 (47%)** | *39.8* | **31.0** | *20.7* | **14.6** |
| Rostr all other | *9/57 (16%)* | **8/46 (18%)** | *20.5* | **16.5** | *3.2* | **2.9** |
| Caud IIn exp | *17/28 (61%)* | **10/31 (32%)** | *43.3* | **64.7** | *23.9* | **20.9** |
| Caud all other | *2/17 (12%)* | **8/47 (17%)** | *40.5* | **24.3** | *4.8* | **4.1** |

The “effective mean” includes all pairs tested for that group, with absence of an EPSP assigned an amplitude of zero

Ford et al. Fig.1

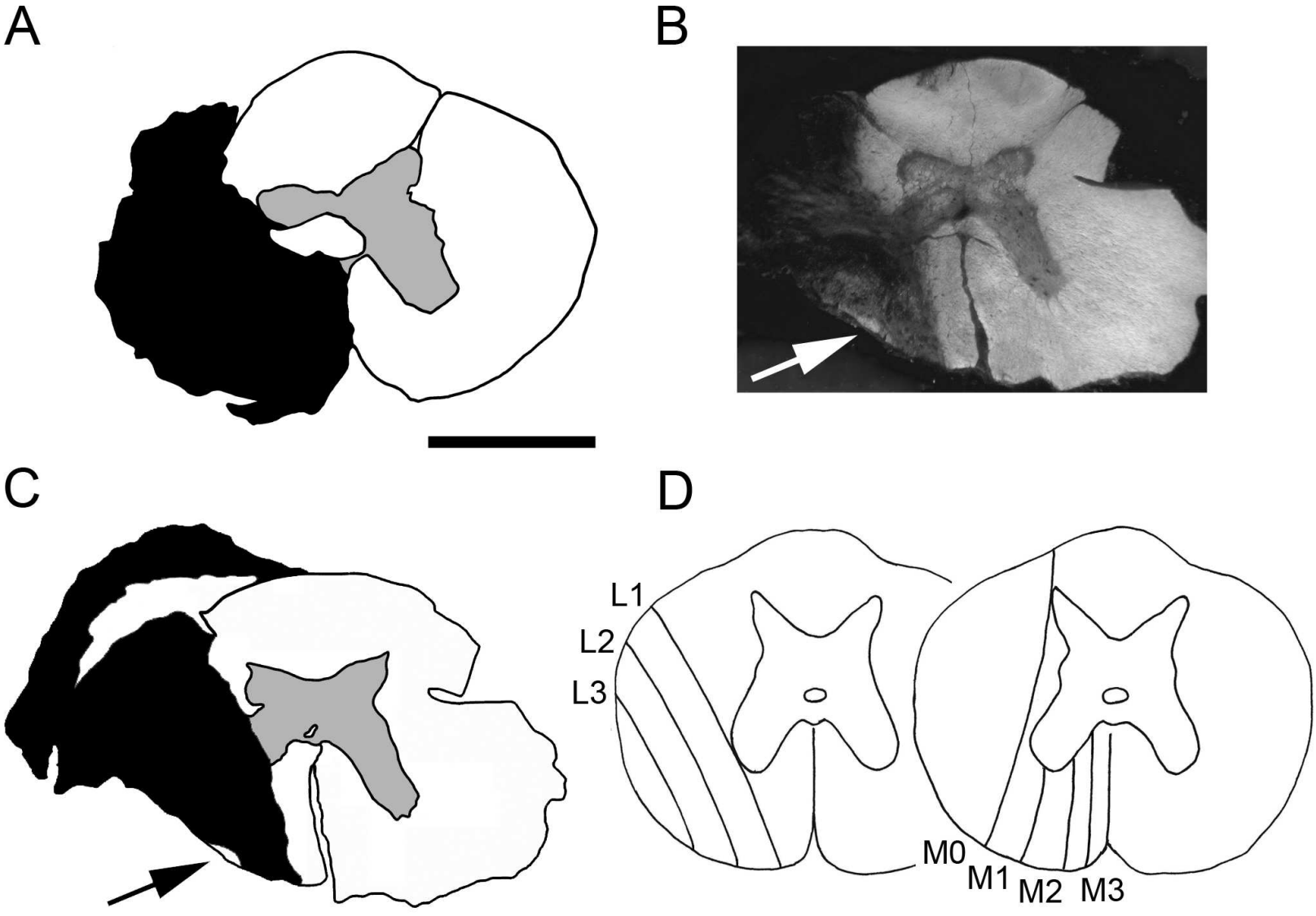

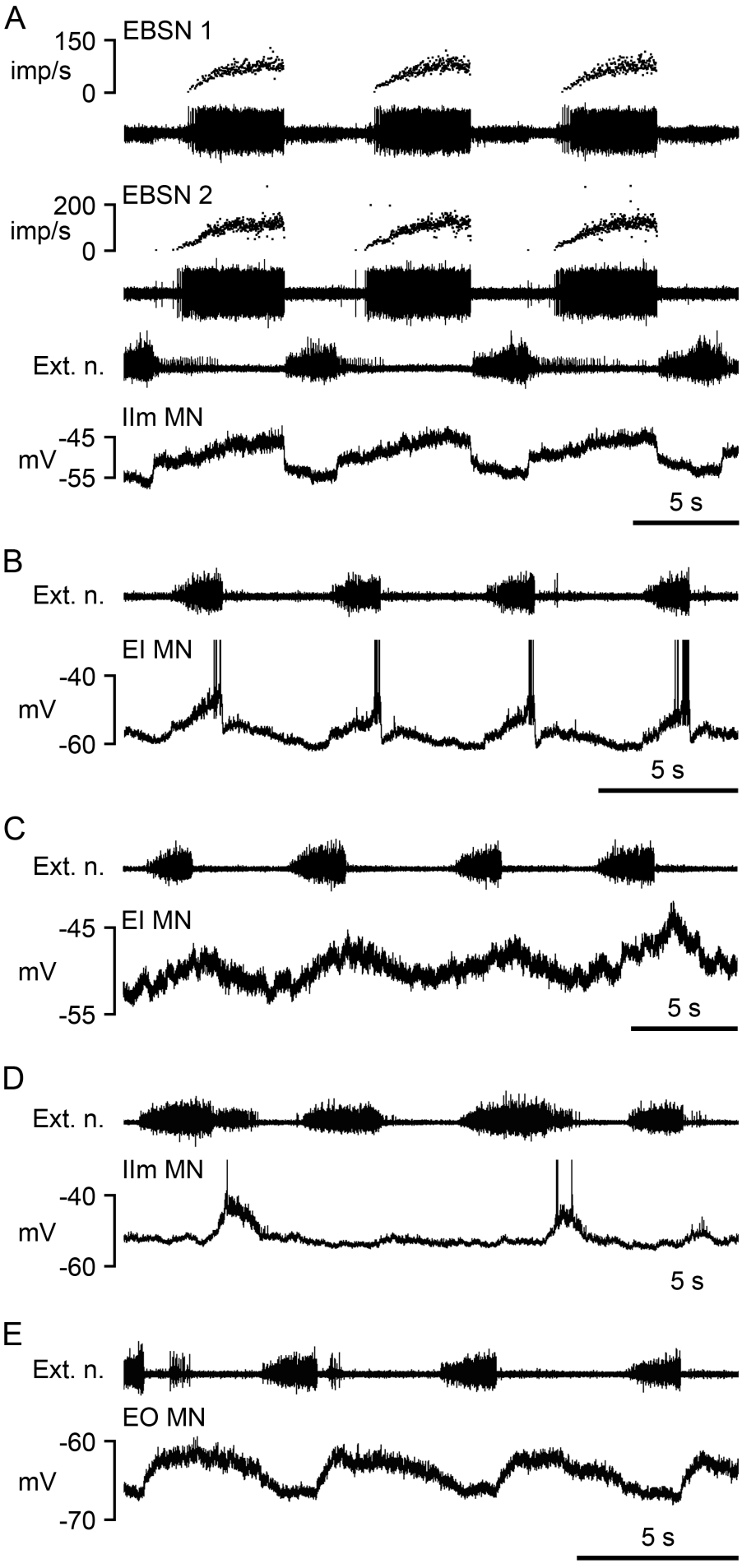
A
EBSN 1
150
imp/s
0
EBSN 2
200
imp/s
0
Ext. n.
IIm MN
-45
mV
-55
5 s
B
Ext. n.
EI MN
-40
mV
-60
5 s
C
Ext. n.
EI MN
-45
mV
-55
5 s
D
Ext. n.
IIm MN
-40
mV
-60
5 s
E
Ext. n.
EO MN
-60
mV
-70
5 s

Ford et al. Fig. 3

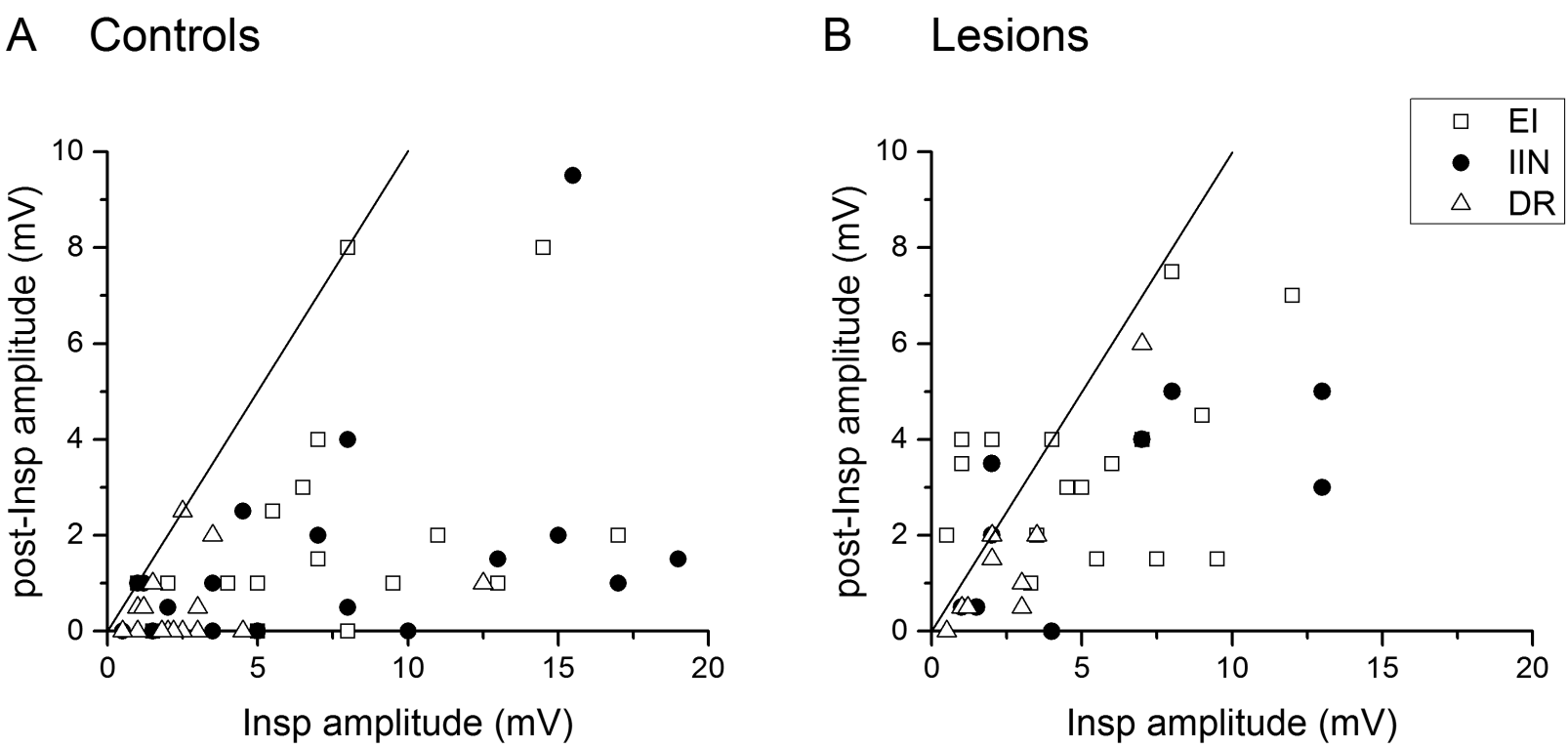

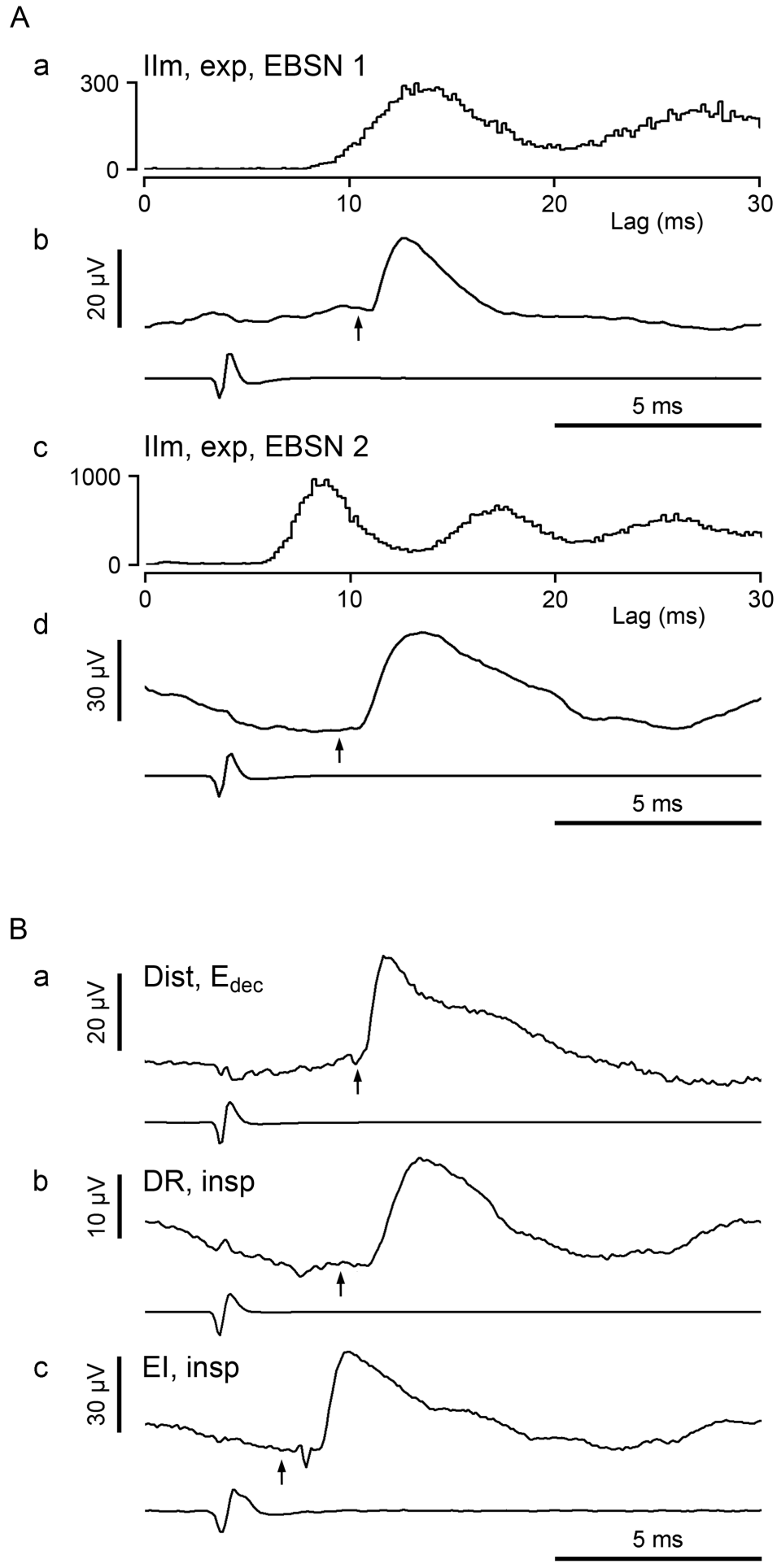
A
a
IIm, exp, EBSN 1
300
0
0
10
20
30
Lag (ms)
b
20 µV
5 ms
c
IIm, exp, EBSN 2
1000
0
0
10
20
30
Lag (ms)
d
30 µV
5 ms
B
a
Dist, $E_{dec}$
20 µV
b
DR, insp
10 µV
c
EI, insp
30 µV
5 ms

Ford et al. Fig 5

| CRDP Category | EPSP Amplitude Distribution | Connectivity | EPSP Amplitude (mean, μV) | EPSP Amplitude (effective mean, μV) | Ramp Amplitude (mean, mV) |
|---|---|---|---|---|---|
| non-Expiratory | 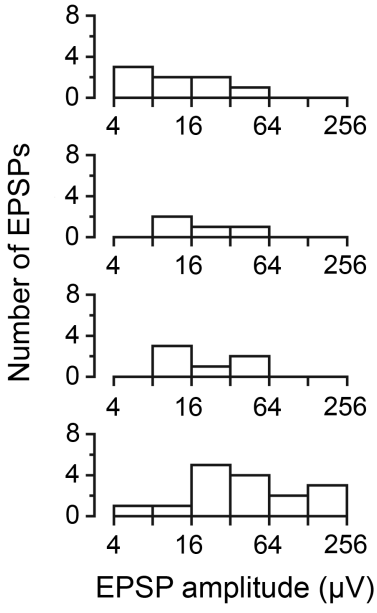 | 8/26 (30.8%) | 16.2 | 5.0 | - |
| Ramp <1mV | | 4/21 (19.1%) | 22.3 | 4.3 | 0.31 |
| Ramp ≥1mV < 2.2mV | | 6/16 (37.5%) | 22.4 | 8.4 | 1.59 |
| Ramp ≥2.2mV | | 16/28 (57.1%) | 58.4 | 33.4 | 4.36 |

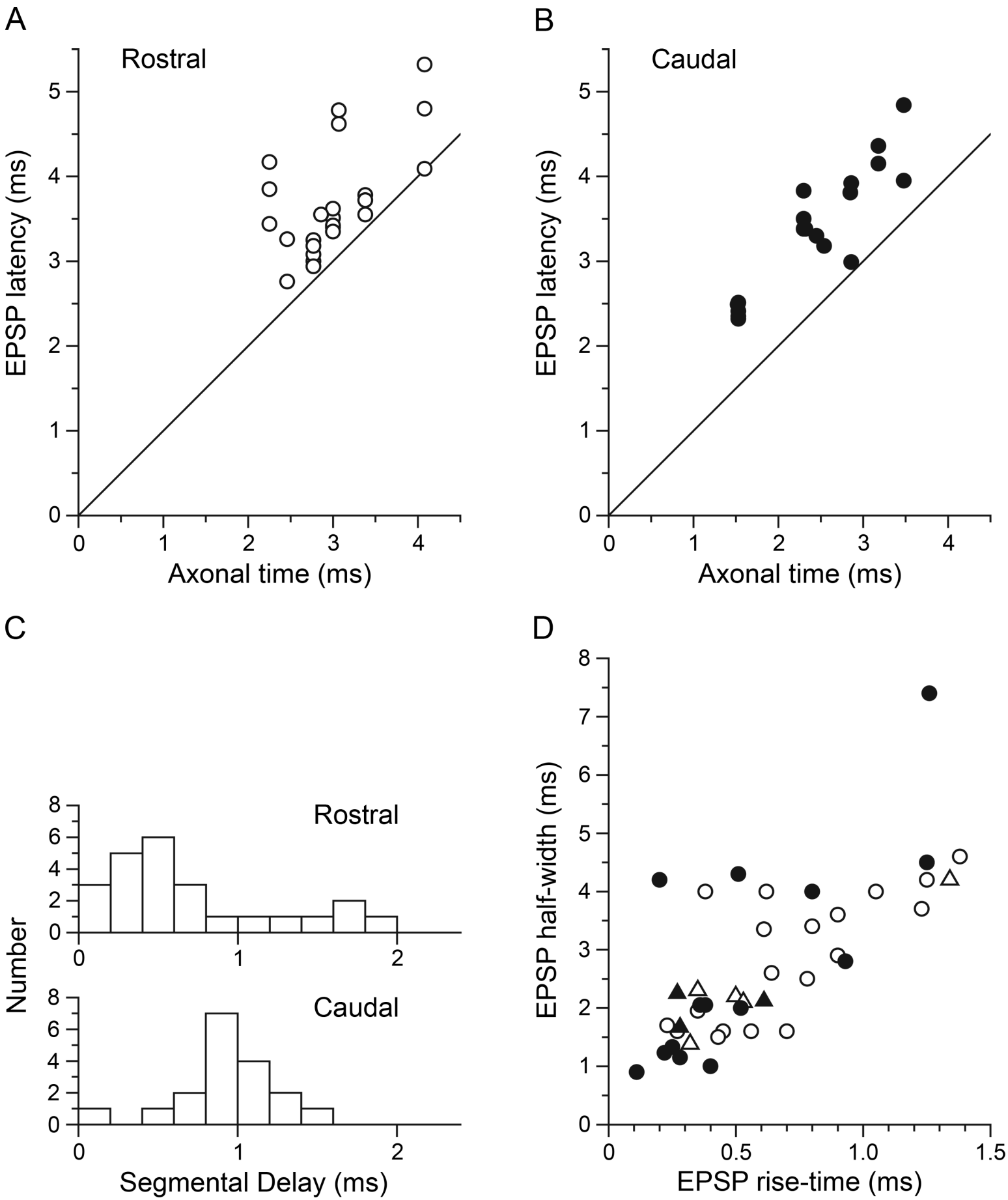
A
Rostral
EPSP latency (ms)
Axonal time (ms)
B
Caudal
EPSP latency (ms)
Axonal time (ms)
C
Rostral
Caudal
Number
Segmental Delay (ms)
D
EPSP half-width (ms)
EPSP rise-time (ms)

Ford et al. Fig. 7